Journal of Power Sources 273 (2015) 118–122

Contents lists available at ScienceDirect

Journal of Power Sources

journal homepage: www.elsevier.com/locate/jpowsour

Short communication

Electrochemical properties of non-nano-silicon negative electrodes prepared with a polyimide binder

Satoshi Uchida, Megumi Mihashi, Masaki Yamagata, Masashi Ishikawa*

Department of Chemistry and Materials Engineering, Faculty of Chemistry, Materials and Bioengineering, Kansai University, 3-3-35 Yamate-cho, Suita 564-8680, Japan

HIGHLIGHTS

- A non-nano-sized Si particle anode is successfully developed with a polyimide binder.
- The strong adhesion of the binder suppresses the electrode structure collapse.
- An electrolyte additive VC is effective for the present systems.
- The Si anode kept 800 mAh g^{-1} discharge in 195 cycles at 1C-rate.
- The conduction-enhanced system kept 800 and 1200 mAh g^{-1} in 300 and 166 cycles at 1C.

ARTICLE INFO

Article history:
Received 4 September 2014
Received in revised form
12 September 2014
Accepted 13 September 2014
Available online 22 September 2014

Keywords:
Si negative electrode
Polyimide binder
μm-Si particles
Li-ion battery

ABSTRACT

We successfully improved the cycle stability of a silicon (Si) negative electrode that consisted of untreated, conventional micro-sized Si particles by applying polyimide (PI) with a low breaking elongation percentage and a high tensile strength as a binder. The strong adhesion of the PI binder suppresses the collapse of the Si negative electrode undergoing the expansion/contraction of Si particles during lithiation/delithiation so that the PI-Si electrode maintains a discharge capacity of 800 mAh g^{-1} during 195 cycles at a current density of 800 mA g^{-1}. The electrodes prepared in this study contain a PI binder of 15 wt.% to maintain the electrode structure. Such a comparatively large amount of PI binder may prevent Li-ion access into Si particles. Nevertheless, the present Si negative electrode with sufficient electronic conductivity maintains a discharge capacity of 800 mAh g^{-1} during 167 cycles even at a high rate (1600 mA g^{-1}). Perhaps the PI binder does not hinder Li-ion access to Si particles. The cell containing a highly porous polyolefin film coated with ceramic as a separator for a facile supply of Li ion from a bulk electrolyte shows excellent cycle stability and maintains a discharge capacity of 800 mAh g^{-1} during 300 cycles.

1. Introduction

Lithium (Li)-ion batteries must become larger and provide greater energy density in the technological stream from internal combustion vehicles to electric vehicles [1]. Even though graphite, which has high electronic conductivity and sufficiently low potential for intercalation/deintercalation of Li ion vs. Li/Li^+, has widely been used as negative electrode material of Li-ion batteries [2,3], it has already reached its theoretical capacity. In other words, it is impossible to increase the specific capacity of negative electrodes with graphite. In recent years, Si has attracted considerable attention as an alternative material to graphite because it has relatively low potential for alloying/de-alloying with Li ion (0.4 V vs. Li/Li^+) and an extremely high theoretical capacity of 4200 mAh g^{-1} ($Li_{4.4}Si$) [4], which is ten times higher than that of graphite. Therefore, drastic improvement in the energy density of Li-ion batteries is expected with Si as a negative electrode material. However, the volume of Si significantly expands (up to approximately 400%) and contracts during lithiation and delithiation [5,6]. As a result, the structure of Si negative electrodes collapses and the capacity decreases rapidly with increasing cycles [7–9]. To solve this problem, modified electrodes using nano-structured Si (e.g., Si nano-particles, Si/carbon (Si/C) nano-composites, and Si nanowires) have been studied because they can reduce the internal

* Corresponding author.
E-mail address: masaishi@kansai-u.ac.jp (M. Ishikawa).

http://dx.doi.org/10.1016/j.jpowsour.2014.09.096
0378-7753/

stress of the electrodes with expansion and contraction on the Si negative electrodes [10–12]. Although the cycle performance of these electrodes significantly improved, the practical use of such nano-Si remains difficult because preparing these materials requires complex processes [10–13].

To apply Si negative electrodes to commercial Li-ion batteries, their cycle stability must be improved by a simple and inexpensive process. Researchers who are attempting to improve the cycle stability of Si negative electrodes should focus not only on active material but also on auxiliary materials that are comprised of negative electrodes. Recently, it has been reported that the cycle stability of Si negative electrodes greatly depends on the type of binders [14,15]. In the refs. [14 and 15], ballmilled SiO and nano-sized Si powder were used as active material. These fine materials require considerable efforts and cost for their mass production. Therefore, our interest is to find a positive binder effect on inexpensive micro-sized Si powder as conventional active material without any complex processes. In this study, we demonstrate improvement in the cycle stability of Si negative electrodes, even using untreated, conventional micro-sized Si particles (μm-Si) by a PI binder with a low breaking elongation percentage and a high tensile strength.

2. Experimental

We prepared Si negative electrodes with a polyimide binder (PI-Si) in a dry room with a dew point of −55 °C. The untreated μm-Si was mixed with acetylene black (AB, Denki Kagaku Kogyo Corp., HS-100) and polyamic acid as precursor of PI in a weight ratio of 80:5:15 or 75:10:15 (the content of PI binder was optimized in terms of the electrode's mechanical strength) with an adequate amount of *N*-methyl-2-pyrrolidone (NMP, Kishida Chemical Co., 99.5%) solvent. The obtained slurry was cast onto a Cu-foil current collector and dried at 80 °C for 2 h in a vacuum oven to remove the NMP. To change the polyamic acid into polyimide by dehydration condensation, the oven temperature was raised to 250 °C and the sample was cooled to room temperature. The PI binder prepared in this study has a relatively low breaking elongation percentage (10%) and high tensile strength (7.5 GPa). We used styrene-butadiene rubber (SBR) as control binder material, which has been widely known as a typical binder for various negative electrodes. Thus we also prepared another Si negative electrode with SBR binder (SBR-Si). The untreated μm-Si was mixed with AB, carboxymethylcellulose, and SBR at a weight ratio of 80:10:5:5 in an adequate amount of deionized water. The obtained slurry was cast onto a Cu-foil current collector and dried at 80 °C for 10 h in a vacuum oven. The prepared electrode sheets were cut into 12-mm diameter disks for electrochemical measurements. The mass loading of Si in the electrodes was approximately 2.0 mg cm^{-2}.

Electrochemical measurements were performed using a two-electrode-type cell assembled in an argon-filled globe box with the prepared Si electrodes, a Li foil (Honjo Metal Corp.) with a 13-mm diameter disk, a 1 M $LiPF_6$ binary electrolyte composed of ethylene carbonate and dimethyl carbonate (1:1 v/v) (Kishida Chemical Co., LBG) including 3 wt.% of vinylene carbonate (VC, Kishida Chemical Co., LBG), and polyolefin porous film or highly porous polyolefin film coated with ceramic as a separator. In this study, we attempted to evaluate a clear-cut effect of the PI binder on the collapse of the electrode structure for the improvement of the cycle stability. Therefore, an effective additive VC was introduced into the electrolyte to inhibit the continuous electrolyte decomposition that is a dominant factor in the cycle performance irrespective of binder.

The charge and discharge measurements were carried out using a galvanostatic charge/discharge unit (Intex Co., BTS2004W). In this paper, we refer to the alloying process of Si with Li (i.e., the direction in which the cell voltage decreases) as the "charge" and the de-alloying process (i.e., the direction in which the voltage increases) as the "discharge". In the initial cycle, the test cells were charged to 5 mV and discharged to 1500 mV with a constant current density of 200 mA g^{-1}. After the second cycle, the test cells were charged to 800 or 1200 mAh g^{-1} as a limited capacity and discharged to 1500 mV at constant current densities of 800–1600 mA g^{-1}. When the cell voltage reached 5 mV before the charge capacity achieved 800 or 1200 mAh g^{-1}, the charge process was terminated.

The surface morphologies of the Si electrodes before and after the cycles were observed using a scanning electron microscope (SEM, Hitachi Co., SU-1500).

3. Results and discussion

Fig. 1(a) and (b) show the SEM image and particle size distribution of the μm-Si particles. The μm-Si's primary particle size extends between 0.3 and 20 μm, and its average particle size is 4.68 μm. In the case of cycling such Si particles, the pulverization of Si particles and the collapse of electrode structure occur with severe volume expansion and contraction of Si particles. As a result capacity degradation occurs rapidly. However, we found that rapid capacity degradation can be suppressed using the present polyimide binder.

Fig. 2(a) and (b) show the charge and discharge curves of the cell including PI-Si and the SBR-Si electrodes. The initial charge capacities of the PI-Si and SBR-Si electrodes at low current density (200 mA g^{-1}) are ca. 2760 and 2870 mAh g^{-1}; there is no significant difference between these values. On the other hand, the initial discharge capacities of the PI-Si and SBR-Si electrodes are ca. 2150 and 1890 mAh g^{-1}; the initial cycle efficiency of the PI-Si electrode

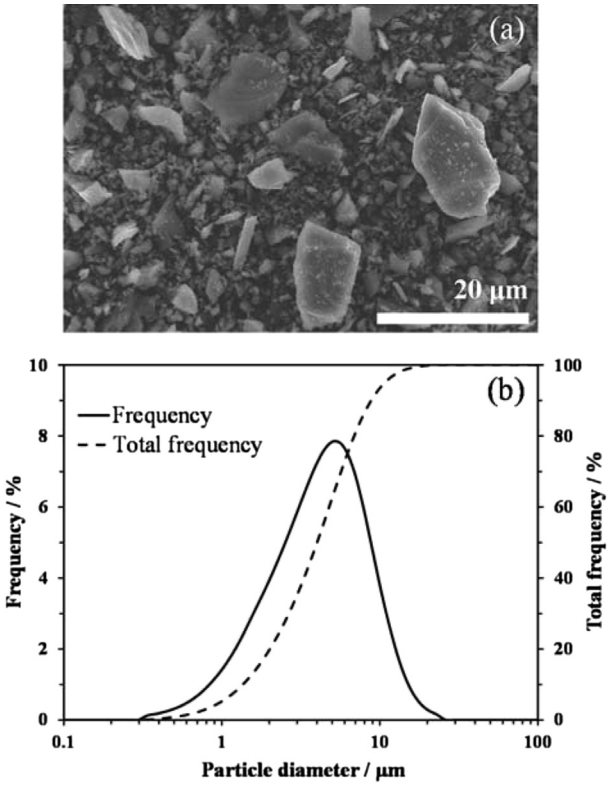

Fig. 1. SEM image (a) and particle size distribution (b) of μm-Si particle.

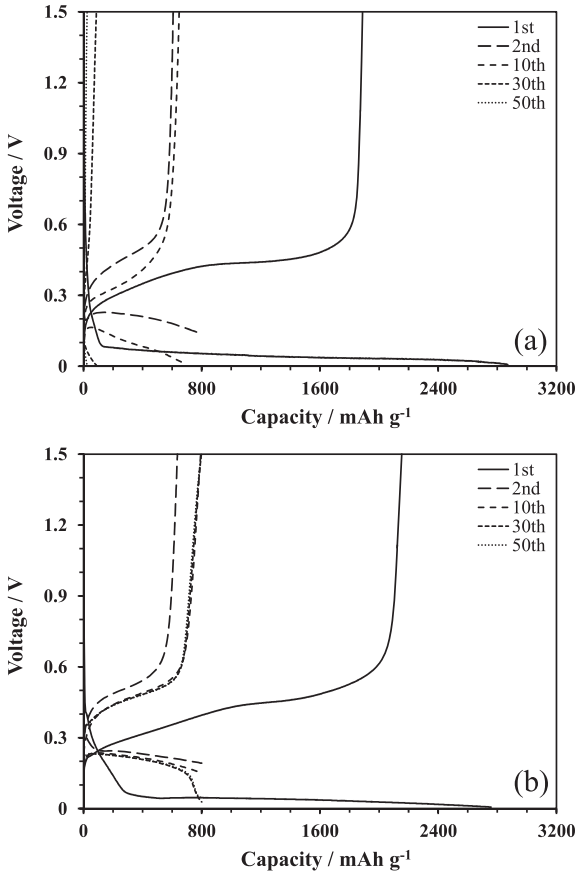

Fig. 2. Charge and discharge curves of cells including PI-Si (a) and SBR-Si (b) electrodes.

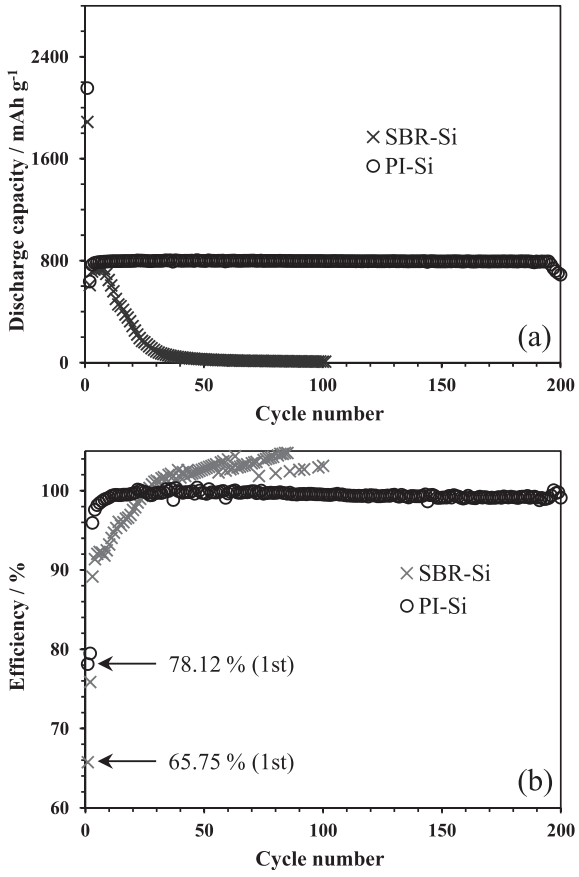

Fig. 3. Discharge capacity (a) and cycle efficiency (b) vs. cycle number of cells including PI-Si and SBR-Si electrodes with limited charge capacity to 800 mAh g^{-1} (after 2nd cycle).

(ca. 77.9%) is significantly higher than that of the SBR-Si electrode (ca. 65.9%). After the 2nd cycle where the charge capacity is limited to 800 mAh g^{-1}, the polarization of the SBR-Si electrode between charge and discharge continues to increase with more cycles, but PI-Si polarization does not; the charge and discharge curves continue to follow almost the same trajectory even after the 30th cycle.

Fig. 3(a) and (b) show the discharge capacities and cycle efficiencies vs. cycle number of the cells including the PI-Si and SBR-Si electrodes where the charge capacity was limited to 800 mAh g^{-1} (after the 2nd cycle). As expected from Fig. 2, SBR-Si's discharge capacity significantly reduced and maintained a discharge capacity of 800 mAh g^{-1} during only a few cycles, while the PI-Si electrode's cycle stability was excellent and maintained a discharge capacity of 800 mAh g^{-1} during 195 cycles. In addition, the cycle efficiency of the PI-Si electrode always maintained high values; the average cycle efficiency from the 11th to 190th cycles was ca. 99.5%. These results mean that the electronic contacts between the Si particles are retained even with Si pulverization due to the repetition of the expansion and contraction of the Si particles.

Fig. 4(a) and (b) show the surface morphologies of the PI-Si and SBR-Si electrodes without cycling and after 10 cycles. Without the cycles, there was no difference between these electrodes except that the PI-Si electrode seemed to be covered in slightly more polymer than the SBR-Si electrode. However, the surface of the PI-Si and SBR-Si electrodes was completely changed after 10 cycles. Many interspaces are confirmed between the Si particles, and the electronic contacts between them are obviously lost. The pulverization of the Si particles hardly occurs in the SBR-Si electrode because the Si particles that lost electronic contacts cannot alloy with Li, significantly reducing their utilization. But pulverization of Si particles does occur on the PI-Si electrode surface. However, the interspaces between the pulverized Si particles were not confirmed, and large cracks are clearly observed. The portions surrounded by these large cracks resemble an island, where the pulverized Si particles are in close contact with each other. The electronic contact between the Si particles on the same island seems to be sufficiently maintained. Since the material density of PI-Si and SBR-Si without the cycles are approximately the same, the above difference in electrode structure after charge and discharge between the PI-Si and SBR-Si electrodes is probably caused by a difference in the properties of the binders. The present PI binder is a very hard polymer with strong adhesion (see the values of its breaking elongation percentage and high tensile strength in Experimental). Even when we peeled the curing tape off the PI-Si electrode surface, the active material layer did not come off completely. The strong adhesion of the present PI binder will probably suppress the collapse of the electrode structure.

The PI-Si electrode prepared in this study contains 15 wt.% of PI binder to suppress the collapse of the relatively large electrode structure. Since a large amount of binder might adversely affect the charge and discharge at high current density, we investigated the cycle performance of the PI-Si electrode at high current density. Fig. 5(a) and (b) show the discharge capacities and cycle efficiencies vs. cycle number of the cells with PI-Si electrodes at a current density of 1600 mA g^{-1} where the charge capacity was limited to 800 mAh g^{-1} (after the 2nd cycle). The electrode, which was

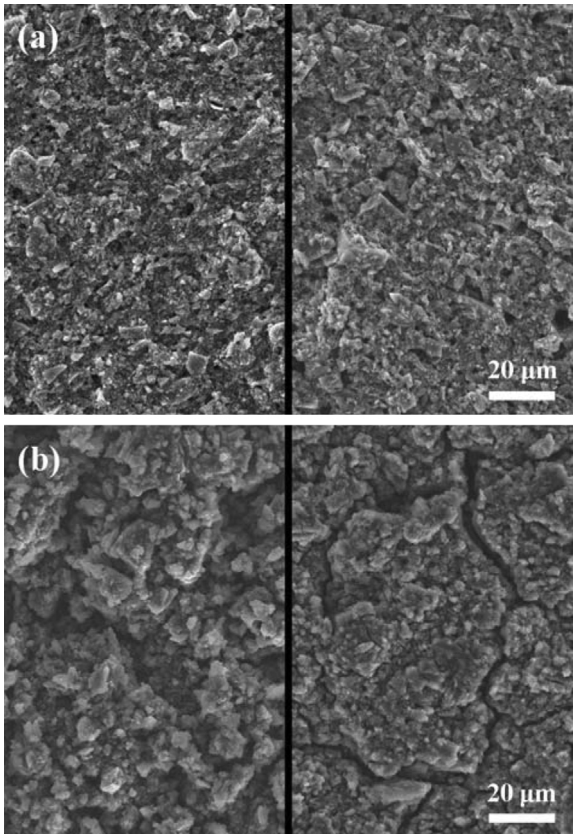

Fig. 4. Surface morphology of PI-Si and SBR-Si electrodes before cycles (a) and after 10 cycles (b). Left images are obtained from SBR-Si electrode and right images from PI-Si electrode.

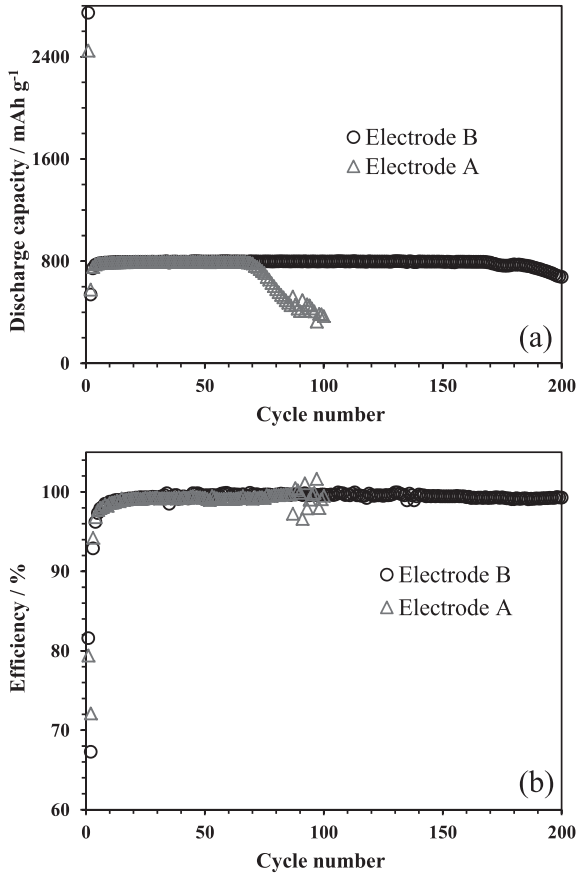

Fig. 5. Discharge capacity (a) and cycle efficiency (b) vs. cycle number of cells including different PI-Si electrodes (Electrode A and B) at current density of 1600 mA g^{-1} with limited charge capacity to 800 mAh g^{-1} (after 2nd cycle).

composed of μm-Si, AB, and PI in a weight ratio of 80:5:15 (Electrode A), maintained a discharge capacity of 800 mAh g^{-1} during only 68 cycles, and the average cycle efficiency of Electrode A from the 11th to the 60th cycles (99.19%) was slightly reduced more than that at a current density of 800 mA g^{-1}. We believe that the causes of the electrode degradation at high current density are inhomogeneous expansion and contraction of the Si particles due to insufficient electronic conductivity in the electrode or the hindrance of Li-ion access to Si particles by a large amount of PI binder. If the former is the major cause, the percentage of AB in the electrode composition should be increased; if the latter is dominant, the percentage of PI in the electrode composition should be decreased because a large amount of PI inhibits Li-ion access to the Si particles. Thus, we prepared another electrode that was composed of μm-Si, AB, and PI in a weight ratio of 75:10:15 (Electrode B) and investigated its cycle performance. Electrode B maintained a discharge capacity of 800 mAh g^{-1} during 167 cycles at a current density of 1600 mA g^{-1} that was as long as the cycle test at a current density of 800 mA g^{-1}. It showed a high average cycle efficiency (ca. 99.5%) from the 11th to 165th cycles. Since the cycle stability in the high current density improved using Electrode B that contained a large amount (10 wt.%) of AB, insufficient electronic conductivity caused the electrode degradation observed at high current density. Therefore, the 15 wt.% PI binder does not hinder Li-ion access to the Si particles.

A facile Li-ion supply to the Si particles also effectively improves the PI-Si electrode's cycle stability because we believe that homogeneous expansion and contraction of Si particles with sufficient electronic conductivity will probably reduce the collapse and improve the cycle stability of the PI-Si electrodes. Thus, we applied highly porous polyolefin film coated with ceramic as a separator for the Li-ion supply from the bulk electrolyte. Fig. 6(a) shows the initial charge and the discharge curves of the cell including Electrode B and the highly porous polyolefin separator coated with ceramic at a low current density (200 mA g^{-1}) without a limitation of the charging capacity. Fig. 6(b) shows its discharge capacities vs. cycle number at current densities 800 and 1200 mA g^{-1} when the charge capacity was limited to 800 and 1200 mAh g^{-1} (after the 2nd cycle). At the initial cycle without any charge capacity limitations, the cell, which includes Electrode B and the highly porous separator, shows a charge capacity of ca. 4000 mAh g^{-1} that is close to the theoretical capacity of Si and significantly higher than that of the cell including a conventional separator (Fig. 2). The corresponding discharge capacity also increases (ca. 3140 mAh g^{-1}) and the initial cycle efficiency is ca. 78.5%, which does not decrease despite an increase in the utilization of Si particles. In addition, the cell including Electrode B and a highly porous separator shows significantly enhanced cycle stability compared to that of the cell with a conventional separator; it maintains discharge capacities of 800 and 1200 mAh g^{-1} during 300 and 166 cycles. The separators do not directly contribute to the charge and discharge reactions, and the separator's role is insulation between the positive and negative electrodes. However, the above results show that different types of separators evidently affect the cycle stability and the utilization of the Si particles, at least when using μm-Si, which seems to depend on the Li-ion conductivity of the separators derived from the porosity and materials.

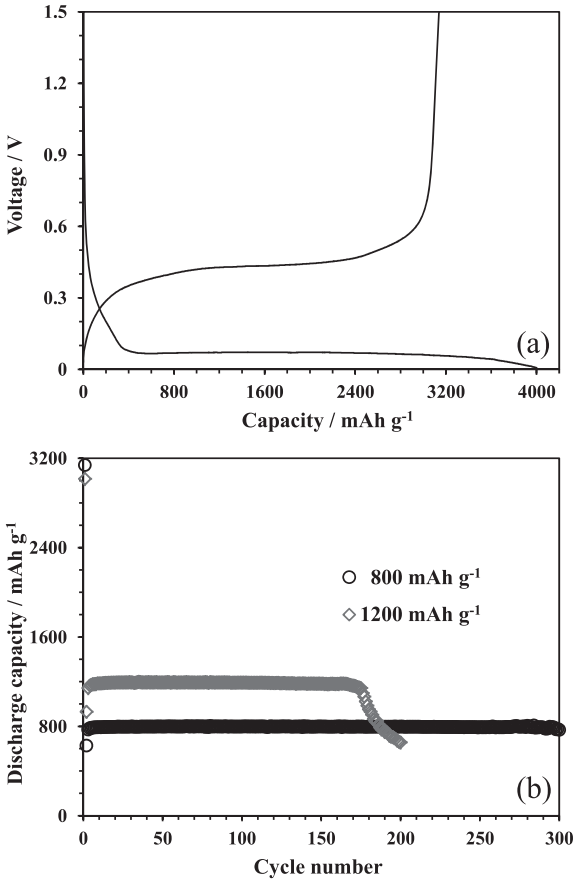

Fig. 6. Initial charge and discharge curves of cell including Electrode B and highly porous polyolefin separator coated with ceramic at low current density (200 mA g^{-1}) without limitation of charge capacity: (a); discharge capacity vs. cycle number at current densities of 800 and 1200 mA g^{-1} with limited charge capacities to 800 and 1200 mAh g^{-1} (after 2nd cycle): (b).

4. Conclusions

We applied a polyimide (PI) binder with a low breaking elongation percentage and a high tensile strength to suppress the collapse of the Si electrode structure and to improve the cycle stability of electrodes composed of untreated, conventional Si particles (μm-Si). The PI-Si electrode maintained a discharge capacity of 800 mAh g^{-1} during 196 cycles at a current density of 800 mA g^{-1}. We were concerned that the relatively large amount of PI binder (15 wt.%) in our electrodes might prevent Li-ion access to the Si particles and adversely affect the cycle stability of the PI-Si electrodes during high-rate operation. However, a PI-Si electrode including 10 wt.% of AB (Electrode B) maintained a discharge capacity of 800 mAh g^{-1} during 167 cycles at a current density of 1600 mA g^{-1}. We found that poor electronic conductivity causes electrode degradation at a high current density, and the PI binder does not essentially hinder Li-ion access to the Si particles. Because the Li-ion supply from the bulk electrolyte also affected the PI-Si electrode's cycle stability and the electronic conductivity, the cells including a highly porous separator maintained discharge capacities of 800 and 1200 mAh g^{-1} during 300 and 166 cycles.

We successfully improved the cycle stability of Si electrodes without using nano-Si by using PI as a binder and found that the porosity and the material selections of the separator that govern Li-ion conduction are crucial. Note that the battery auxiliary components, which are not directly involved in the charge and discharge reactions, such as binders and separators, significantly affect the battery performances of Si negative electrodes. We believe that effectively using these components will greatly contribute to the practical applications of Si negative electrodes.

References

[1] E. Karden, S. Ploumen, B. Fricke, T. Miller, K. Snyder, J. Power Sources 168 (2007) 2.
[2] M. Winter, J.O. Besenhard, M.E. Spahr, P. Novak, Adv. Mater. 10 (1998) 725.
[3] D. Aurbach, B. Markovsky, I. Weissman, E. Levi, Y. Ein-Eli, Electrochim. Acta 45 (1999) 67.
[4] R.A. Huggins, J. Power Sources 81-82 (1999) 13.
[5] B.A. Boukamp, G.C. Lesh, R.A. Huggins, J. Electrochem. Soc. 128 (1981) 725.
[6] L.Y. Beaulieu, K.W. Eberman, R.L. Turner, L.J. Krause, J.R. Dahn, Solid-State Lett. 4 (2001) A134.
[7] Y. Oumellal, N. Delpuech, D. Mazouzi, N. Dupre, J. Gaubicher, P. Moreau, P. Soudan, B. Lestriez, D. Guyomard, J. Mater. Chem. 21 (2011) 6201.
[8] J.H. Ryu, J.W. Kim, Y.E. Sung, S.M. Oh, Solid-State Lett. 7 (2004) A306.
[9] S. Pal, S. Damle, S. Patel, M.K. Dutta, P.N. Kumta, S. Maiti, ECS Trans. 41 (2012) 87.
[10] H. Kim, M. Seo, M.H. Park, J. Cho, Angew. Chem. Int. Ed. 49 (2010) 2146.
[11] C.K. Chan, H. Peng, G. Liu, K. Mcilwrath, X.F. Zhang, R.A. Huggins, Y. Cui, Nat. Nanotechnol. 3 (2008) 31.
[12] L.F. Cui, Y. Yang, C.M. Hsu, Y. Cui, Nano Lett. 9 (2009) 3370.
[13] C.K. Chan, R. Ruffo, S.S. Hong, R.A. Huggins, Yi Cui, J. Power Sources 189 (2009) 34.
[14] S. Komaba, K. Shimomura, N. Yabuuchi, T. Ozeki, H. Yui, K. Konno, J. Phys. Chem. C 115 (2011) 13487.
[15] I. Kovalenko, B. Zdyrko, A. Magasinski, B. Hertzberg, Z. Milicev, R. Burtovyy, I. Luzinov, G. Yushin, Science 334 (2011) 75.